Separation Science and Technology
Publication details, including instructions for authors and subscription information:
http://www.informaworld.com/smpp/title~content=t713708471

Use of Electrodialysis to Remove Acid, Salt, and Heavy Metal Mixtures from Aqueous Solutions

D. A. Rockstraw[a]; J. F. Scamehorn[b]
[a] CHEMICAL ENGINEERING DEPARTMENT, NEW MEXICO STATE UNIVERSITY LAS, CRUCES, NEW MEXICO, USA [b] SCHOOL OF CHEMICAL ENGINEERING & MATERIALS SCIENCE, THE UNIVERSITY OF OKLAHOMA, NORMAN, OKLAHOMA, USA

To cite this Article Rockstraw, D. A. and Scamehorn, J. F.(1997) 'Use of Electrodialysis to Remove Acid, Salt, and Heavy Metal Mixtures from Aqueous Solutions', Separation Science and Technology, 32: 11, 1861 — 1883
To link to this Article: DOI: 10.1080/01496399708000742
URL: http://dx.doi.org/10.1080/01496399708000742

SEPARATION SCIENCE AND TECHNOLOGY, 32(11), pp. 1861–1883, 1997

Use of Electrodialysis to Remove Acid, Salt, and Heavy Metal Mixtures from Aqueous Solutions

DAVID A. ROCKSTRAW*
CHEMICAL ENGINEERING DEPARTMENT
NEW MEXICO STATE UNIVERSITY
LAS CRUCES, NEW MEXICO, USA

JOHN F. SCAMEHORN
SCHOOL OF CHEMICAL ENGINEERING & MATERIALS SCIENCE
THE UNIVERSITY OF OKLAHOMA
NORMAN, OKLAHOMA, USA

ABSTRACT

The effect of solution composition on the electrodialysis design parameters of overall current efficiency and apparent stack resistance for mixtures of acids, monovalent salts, and divalent metals is discussed. Current efficiency was observed to be dependent upon ion valence and independent of the nature of the ionic specie for the membrane system under investigation. Under many conditions, simple linear mixing rules fail to predict these design parameters, particularly for systems at low pH, or when the electrolyte concentration gradient across the membrane is large. However, under commercially desirable operating conditions of high current efficiency, linear mixing rules will predict system performance for mixed ion systems composed of ions of differing valences.

APPLICATIONS OF ELECTRODIALYSIS

Electrodialysis (ED) is a membrane-based separation process in which the partial separation of the electrolytic components of an ionic solution is induced by an electric current (1). Electrodialysis has found industrial use in such diverse applications as brackish water desalination (2), acid recovery (3, 4), corn sugar solution demineralization (5), photographic

* To whom correspondence should be addressed.

emulsion preparation, radioactive solution concentration (5), heavy metal recovery from plating rinse waters (6), and mining mill process water treatment (7). ED has recently been considered for acidic catalyst synthesis (8), concentration of fermentation broths containing sodium lactate (9), reprocessing of salt regenerates from nuclear power plant water purification systems (10), metal reclamation from plating industry sludges (11), treatment of synthetic antibiotic intermediates (12), and boron removal from the primary cooling loop effluents of pressurized water reactors (13). Variants of the basic electrodialysis process are also being investigated to solve industrial needs, including use of bipolar membranes (14, 15) for conversion of salts into their respective acids and bases (16), and for citric acid separation (17); use of current reversal in the presence of lime (18) applied to the treatment of fertilizer manufacture process effluents (19); and nonaqueous solvent electrodialysis for the production of sodium methoxide from methanol and sodium chloride (20).

The removal of electrolytes in multicomponent systems from aqueous streams is considered in this work. Theoretical understanding of ionic transport for binary systems has been considered in previous works (21, 22). These studies are of limited use experimentally due to the many simplifying assumptions required to solve the governing equations. A complete solution of the transport phenomena for a single salt system has been performed that includes the processes of migration, electroosmosis, diffusion, osmosis, hydraulic flow, streaming potential, and membrane potential (23).

BASIC OPERATING PRINCIPLES OF ELECTRODIALYSIS

A schematic diagram for an electrodialysis membrane stack is shown in Fig. 1. The stack consists of a series of alternating cation-exchange and anion-exchange membranes, each separated by a spacer through which the solutions flow. When an electrical potential is applied across the stack, cations in solution begin to migrate toward the cathode, and anions toward the anode. When a cation encounters a cation-exchange membrane, it will pass freely to the other side. As the cation continues to migrate, it subsequently encounters an anion-exchange membrane. The electrostatic repulsion between the cation and the fixed cationic charges within the anion-exchange membrane resist the tendency for the cation to travel further toward the cathode. When the similar phenomenon is considered for the migrating anions, the net effect is that each compartment bounded on the cathode side by an anion-exchange membrane becomes increasingly enriched in electrolyte (concentrate stream). The compartments

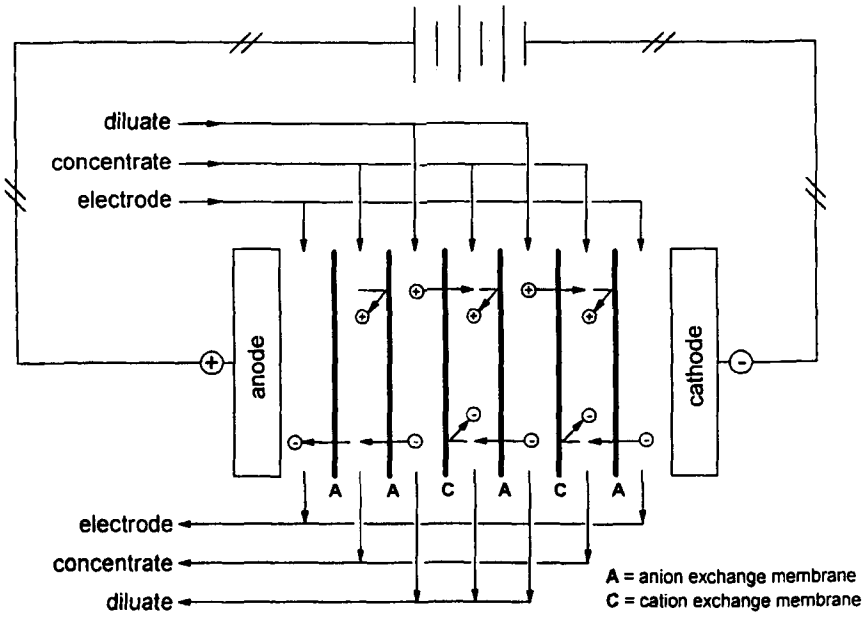

FIG. 1 Schematic diagram of experimental electrodialysis membrane stack.

bounded on the cathode side by a cation-exchange membrane become increasingly depleted in electrolyte (diluate stream).

RELATIONSHIP OF DESIGN VARIABLES TO PROCESS ECONOMICS

Electrodialysis has been shown to be more cost competitive than ion-exchange for feed solution concentrations above 500 g/L, and the separation scheme of choice over reverse osmosis for feeds below 5000 ppm (24). When an electrodialysis application is being considered, the two design parameters of concern are the overall current efficiency and the apparent stack resistance (1).

The *overall current efficiency* (η_I) is the net transfer of chemical equivalents from the diluate to the concentrate divided by the net passage of electrical equivalents across the membrane stack over some interval of time. The overall current efficiency is calculated from a material balance on the membrane stack and can be based on the conditions that exist in the diluate or the concentrate. Overall current efficiencies (η_I) calculated

in this work are diluate-based and are described by

$$\eta_I = \left\{\frac{FV_D\Delta C_D}{nI}\right\}_{\Delta t} \tag{1}$$

where F is Faraday's constant, V_D is the volume of diluate contained in the experimental unit, ΔC_D is the change in diluate electrolyte concentration in units of normality over time interval Δt, n is the number of cell pairs present in the stack, and I is the number of electrical equivalents transferred during the time interval Δt.

The *apparent stack resistance* is the sum of all electrical resistance across the stack. Contributions to the apparent stack resistance include the membranes, the solutions, and the electrode reactions (both thermodynamic electrical potential and overpotential). Resistances are in series configurations, and are thus additive.

Solution contributions to the apparent stack resistance are dependent on solution flow rates, solution resistivities, and membrane spacing. Under turbulent conditions as found in tortuous path spacers, liquid phase mass transfer resistance becomes negligible. Solution resistivity is inversely related to concentration; thus, resistance contributions from dilute solutions are much higher than those due to the concentrated streams.

Area specific apparent stack resistances (R_a) were calculated applying Ohm's law to the membrane as defined by

$$R_a = \frac{V_a A_\pi}{ni} \tag{2}$$

where A_π is the effective cell pair area (that area exposed to solution flow), i is the current, and V_a is the total electrical potential applied to the membrane stack.

The design variables of overall current efficiency (η_I) and apparent stack resistance (R_a) are studied because each has an impact on the costs associated with the installation and operation of a commercial electrodialysis unit (25). Capital costs are approximately proportional to the required effective cell pair area per unit flow rate (α):

$$\alpha \propto -\frac{nFR_a\Delta C_D}{V_\pi \eta_I} \tag{3}$$

where V_π is the apparent stack potential per cell pair and ΔC_D is the total change in concentration (in equivalents) of the diluate stream during the demineralization.

Operating costs are dominated by the costs associated with energy requirements per unit volume of feed processed (β):

$$\beta \propto -\frac{V_\pi F \Delta C_D}{\eta_l} \tag{4}$$

Both α and β are inversely related to the overall current efficiency, while α is directly proportional to the apparent stack resistance. It is thus desirable to operate at high current efficiency and low stack resistance. Since the applied voltage (V_π) is inversely proportional to the effective cell pair area and directly proportional to the energy demand, the applied voltage can be used as an optimization variable between these cost-determining parameters.

PHYSICAL LIMITATIONS OF ELECTRODIALYSIS

Overall current efficiencies of less than unity are due to a number of contributing factors: 1) the membranes may not have a permselectivity of unity and therefore allow passage (intrusion) of the co-ion; 2) parallel currents may exist across the membrane stack manifold (current leakage); 3) at high current densities or low solute concentrations, hydrogen and hydroxide ions present in the aqueous media begin to participate in the current carrying process (transport by water dissociation ions); and 4) the concentration gradient across a membrane separating the diluate and concentrate compartments drives a diffusive flux of electrolyte back into the diluate (counterion backdiffusion). For many of the conditions used here, neither water dissociation ion transport nor current leakage are significant as evidenced by the ability to achieve high current efficiencies even for concentrated electrolyte.

The applied stack voltage was held constant during the batch experiments. The electrical potential gradient is the driving force for the migration of species from the diluate streams, thus providing a constant driving force for the separation. Electrolyte concentration gradients across the membranes increase, thus increasing the driving force for counterion backdiffusion. The effect of these opposing driving forces (constant electrical gradient and increasing concentration gradient) is that net counterion transport rate across the membrane from the diluate to the concentrate decreases and, hence, current efficiency decreases during the batch separation.

EQUIPMENT AND EXPERIMENTAL DESIGN

The membrane stack configuration used in this study consisted of two cell pairs and an isolating compartment. The isolating compartment allows a different cation to be present in the electrode stream to prevent the

reduction of metals at the electrode surface. Metal reduction on the electrode leads to a reduction in the performance of the electrodialysis unit due to an increase in electrical resistance. Tortuous path spacers were used in this work.

The membranes for this study were Ionics 61-CZL-386 (cation-exchange membranes) and 103-QZL-386 (anion-exchange membranes). These membranes are made from polystyrene with polydivinylbenzene crosslinks as a polymer matrix on a modacrylic reinforcing fabric. Cation-exchange sites are sulfonate groups, while anion-exchange sites are quaternary ammonium groups. These membranes are homogeneous with 220 cm^2 of effective cell pair area. Average pore diameter is 15–20 Å. The electrode materials were platinum-coated columbium for the anode and hastelloy for the cathode.

Figure 2 is a schematic of the experimental unit used in this work. This unit is a modified version of the Ionics Chemomat Stackpack. During operation, the diluate, the concentrate, and the electrode streams were pumped from their holding tanks through the membrane stack. Effluents from the stack were then returned to their originating reservoir. Consequently, the process involves the flow of three independent solutions. During an experimental run, the diluate tank becomes increasingly dilute in electrolyte, the concentrate tank becomes increasingly concentrated

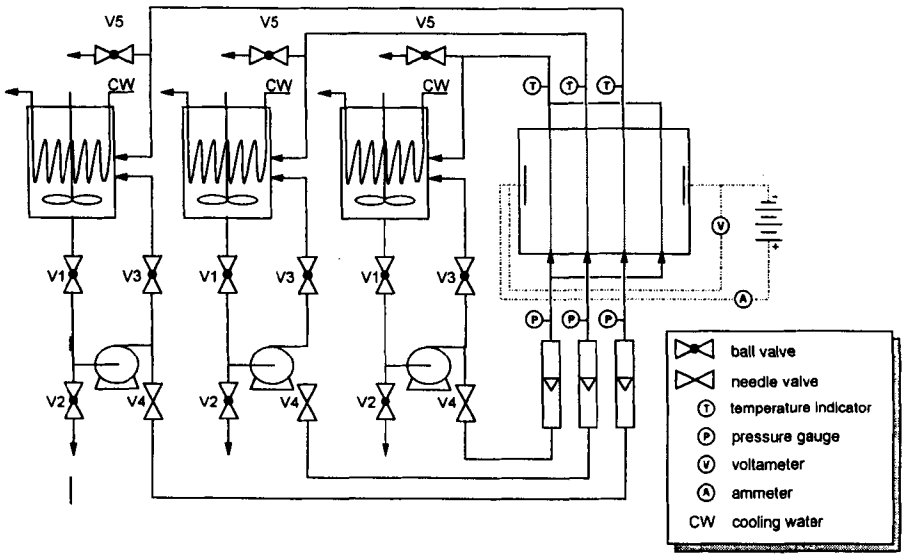

FIG. 2 Schematic diagram of experimental electrodialysis process unit.

in electrolyte, and the electrode stream does not change substantially in composition.

Electrode solutions used in this work were of two types, depending upon the common anion used with the studied solutions. For systems involving chloride as the common anion, the electrode stream was an aqueous 0.2 M NaCl solution, with the pH adjusted to 2.0 with HCl. When sulfate was used as the common anion, an aqueous 0.135 M Na_2SO_4 solution was used in the electrode reservoir with the pH adjusted to 2.0 using H_2SO_4. These concentrations were selected to reduce the contribution that the electrode streams make to the apparent stack resistance, yet ensuring that the electrode stream resistance contribution to the stack resistance was consistent between experimental runs having different anions. These requirements were satisfied in that at the indicated concentrations, these electrode solutions have high equivalent conductivities and therefore low electrical resistances (relative to the diluate streams). Also, these two solutions have similar conductivities at 25°C (26) and their relative contributions to the apparent stack resistance are thus approximately equal.

The unit was operated at a temperature of 78°F, with an applied voltage of 4 V/cell pair. Stream flow rates were set at 0.235 L/min, with line pressures of 15 psig. These operating conditions and ion systems are the same as those reported by Scamehorn and coworkers (3, 27), allowing a direct comparison to those results.

Sample concentrations were determined using a Varion SpectrAA-20 atomic absorption spectrophotometer. Hydrogen ion concentrations were measured using an Orion 7OIA/digital Ionalyzer, with a Fisher Scientific pH electrode (#13-639-3) and a calomel reference electrode (#13-639-52). All acids and solutes used were reagent grade. Water was distilled and deionized prior to use.

NERNST–PLANCK TRANSPORT IN ELECTRODIALYSIS

To gain insight into the expected behavior of mixed systems of electrolytes, a qualitative analysis of the fundamental equations governing the systems is considered.

Ionic mass transfer toward an electrode in a system as an electrodialysis cell will include electrically driven migration ($\mathbf{J}_\phi$), diffusion ($\mathbf{J}_c$), and convection ($\mathbf{J}_v$) driving forces. Each of these transport modes is included respectively in the terms of the *Nernst–Planck* equation:

$$\mathbf{J}_k = \mathbf{J}_c + \mathbf{J}_\phi + \mathbf{J}_v = D_k \nabla C_k - \frac{z_k F}{RT} D_k C_k \nabla \phi + C_k \mathbf{v} \qquad (5)$$

where $\mathbf{J}_k$ is the flux of species k, D_k is the diffusion coefficient, ∇C_k is the gradient of the concentration, ∇_ϕ is the gradient of the electrical potential (the differential change in potential with respect to a differential change in distance), z_k and C_k are the valence and concentration of specie k, respectively, and $\mathbf{v}$ is the solution velocity. The total flux of electrolyte is the sum of the individual species fluxes.

In the case of transport across a membrane, the convective term ($\mathbf{J}_v$) is negligible, and the expression can be reduced as in Eq. (6). The concentration and potential gradients (ΔC_k and $\Delta\phi$) have opposite signs, thus these terms represent the opposing diffusion and electrically driven migration driving forces.

$$\mathbf{J}_k = \mathbf{J}_c + \mathbf{J}_\Phi = -D_k \nabla C_k - \frac{z_k F}{RT} D_k C_k \nabla\phi \tag{6}$$

In terms of functional dependencies of the species fluxes on system concentrations, the potential driven flux ($\mathbf{J}_\Phi$) is observed to be a function of diluate concentration, while the diffusive flux ($\mathbf{J}_C$) is a function of the concentration gradient across the membrane (ΔC). Under typical electrodialysis operating conditions, $C_C \gg C_D$, and thus $\Delta C \approx C_C$, thus the diffusive flux is dependent only upon the concentrate concentration.

The instantaneous current efficiency ($\Delta t \rightarrow 0$) can be considered as the ratio of the sum of species fluxes to the rate of electrical charge transfer (both expressed in eq/cm^{2}s);

$$\eta_I = \sum_n \eta_k^\circ = \frac{\sum_u (z_k J_k)}{(i/FA_\pi)} \tag{7}$$

where the flux of electrolyte is summed over the n electrolytes being transported from the diluate to the concentrate. The instantaneous current efficiency is calculated from consecutive samples of a batch separation as an estimate of the near-steady-state conditions that would exist for a continuous process at the same operating conditions.

This indicates that the current efficiency of a system of mixed ions (η_I) may be predictable when water transport and dissociation are negligible based on the species concentrations in the diluate and concentrate streams and known current efficiencies of the individual species operating under similar conditions (η_i°).

The Nernst–Planck equation provides the necessary qualitative understanding of the process stream concentrations that become dominant in the limiting cases of high and low current efficiency (where one of the two driving forces being considered begins to dominate the transport of species across the membrane). In these cases the functional relationship

describing that driving force provides insight to the important system parameters needed to quantitatively predict the expected current efficiency.

In the first limiting case where current efficiencies approach unity, the diffusive flux of ions across the membrane from the concentrate to the diluate (backdiffusion) becomes negligible ($\mathbf{J}_C \approx 0$). Under these circumstances, the flux from the diluate to the concentrate is due to the electrically driven migration driving force:

$$\mathbf{J}_k = \mathbf{J}_\phi = -\frac{z_k F}{RT} D_k C_k \nabla\phi \tag{8}$$

The electrolyte fluxes are thus independent of the concentrate stream concentration, as C_k is evaluated at diluate conditions near the membrane. The species fluxes and thus the instantaneous current efficiency (η_I) for a mixed component system may be considered a function of the species' diluate concentrations ($x_i C_D$), and the pure component current efficiencies (η_i^0), where the "chemical equivalent fraction" of species "i" in solution is:

$$\chi_i = \left\{ \frac{\text{chemical equivalents of cation } i}{\text{total chemical equivalents of all cations}} \right\} \tag{9}$$

For the limiting case in which the current efficiency approaches zero, the net ionic flux across the membrane nears zero ($\Sigma \mathbf{J}_k \rightarrow 0$). In this case, the driving forces for diffusion and migration are equal;

$$\mathbf{J}_C = \mathbf{J}_\phi \quad \text{or} \quad D_k \nabla C_k = -\frac{z_k F}{RT} D_k C_k \nabla\phi \tag{10}$$

The instantaneous current efficiency for this situation is controlled by both the concentrate and the diluate concentrations. Other transport processes such as water transport become significant under these conditions, and the usefulness of a simple correlation for prediction is expected to be of limited use.

CORRELATION OF MIXED SYSTEM BEHAVIOR

In an attempt to describe the behavior of these mixed component systems using this qualitative knowledge of the Nernst–Planck equation while avoiding the mathematical complications of the electrochemical transport process (28), linear mixing rules for overall current efficiencies are posed, based exclusively on the bulk liquid equivalent fractions of each component in the system and the measured single component instantaneous current efficiencies for those species. Such simple expressions, if found to

be applicable, would be of great value to an engineer screening the economics of potential applications of electrodialysis to mixed component systems in that it would allow the selection of an operating current efficiency for a proposed unit based on limited information available in the literature. These mixing rules are linear interpolations between the curves of the pure component current efficiencies (η_i°):

$$\eta_I^{mix}(C_{t,D}, C_{t,C}) = \sum_i [x_{i,D}\eta_i^\circ(C_{t,D}, C_{i,C} = C_{t,C})] \quad (11)$$

$$\eta_I^{mix}(C_{t,D}, C_{t,C}) = \sum_i [x_{i,C}\eta_i^\circ(C_{t,D}, C_{i,C} = C_{t,C})] \quad (12)$$

where η_I^{mix} is the overall instantaneous current efficiency for the mixed electrolyte system at a total normal diluate concentration of $C_{t,D}$ and a total normal concentrate concentration of $C_{t,C}$, $X_{i,D}$ is the equivalent fraction of cation "i" in the diluate stream of the mixed system, $x_{i,C}$ is the equivalent fraction of cation "i" in concentrate stream of the mixed system, and η_i° is the overall instantaneous current efficiency of the pure component "i" at the same concentration as the mixed system being investigated with respect to both the diluate ($C_{i,D}$) and the concentrate ($C_{i,C}$) streams.

Equation (11) assumes that η_i^{mix} is dictated by the nature of the diluate and the diluate composition, while Eq. (12) assumes that it is dictated by the nature of the concentrate and the concentrate composition. Hence, interpolations from Eq. (11) are referred to as "diluate-based" and from Eq. (12) as "concentrate-based."

Based on the evaluation of the Nernst–Planck equation, it is shown that the diluate-based linear mixing rule (Eq. 11) gives reasonable approximations of the instantaneous current efficiency of the system in commercially desirable operating regions. The resulting approximations are useful for rapid determination of feasibility for treatment of mixed component streams (25).

RESULTS OF BATCH ELECTRODIALYSIS SEPARATIONS FOR MIXED ION SYSTEMS

Cations used in this study were H^+, Na^+, Cd^{2+}, Mg^{2+}, and Zn^{2+}, and anions were Cl and SO_4^{2-}. Experimental results are presented for overall current efficiency for systems containing a number of divalent metals (Fig. 3), for salt/metal systems (Fig. 4–6), for acid/metal systems (Fig. 7), for an acid/salt system (Fig. 8), and for acid/salt/metal mixed systems (Fig.

9). Apparent stack resistances are shown (Figs. 10 and 11) for a number of the runs performed. The design variables (η_I and R_A) are plotted against diluate concentration. Since diluate concentration decreases during the course of a batch run, the progress of a run can be observed by following the curves from high to low current efficiencies.

Figures presenting experimental current efficiency results contain a significant amount of information. Results are presented in a format to provide direct comparison between the design variables of pure systems and those of mixed systems. References made to "salt systems" imply *monovalent cation systems* (as the sodium system studied here), while references to "metal systems" imply *divalent cation systems*. Pure component data used in the figures are from previous work for acid ($X_H = 1$) and salt systems ($X_{Na} = 1$) (3), and for metal systems ($X_{Cd} = 1$) (27).

The equivalent fraction of any species in the diluate changes during a batch separation. Runs were designed with the initial diluate concentration at least an order of magnitude below the initial concentrate concentration. The concentration of each ionic specie in the concentrate stream thus varies by less than 1% during the run, and for the purposes of this analysis can be considered constant. Although hydrogen ion is always present in solution, unless acid is added to the system, the hydrogen ion concentration at neutral pH is too low to have a significant effect on the results and is ignored.

Figure 3 indicates that the nature of a divalent metal solute has no measurable effect on the overall current efficiency for those ions studied. This figure presents the results obtained for systems containing three different divalent ions (cadmium, zinc, and magnesium), and one mixed system composed of all three species. The co-ion used for all systems in this figure was SO_4^{2-}. The nature of the divalent solute does not affect the resulting current efficiencies under the conditions tested. Steric hindrances that would tend to reduce the current efficiency for the larger ions by reducing ionic mobility are thus negligible for the ions and membranes studied in this system. The current efficiency is a function only of the solution concentrations and the valence of the species being transferred, consistent with simplifications applied to the Nernst–Planck equation earlier. The result makes the prediction of current efficiencies for divalent mixtures simple as one may use the experimental results from a pure component system to predict the performance of a mixed system, or to predict the performance of another divalent metal system.

Figure 4 shows the current efficiencies for the salt/metal system with only enough acid present to prevent fouling of the membranes caused by metal precipitates. The results of previous work (27) indicate that with all operating conditions equal, the divalent cadmium system results in higher

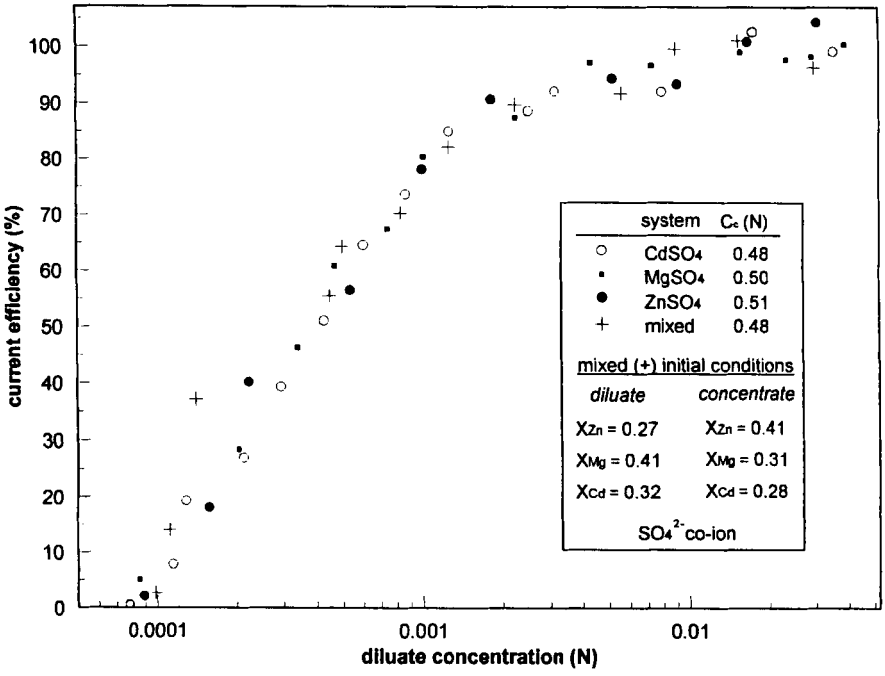

FIG. 3 Effect of diluate concentration on instantaneous current efficiency for divalent metal systems.

current efficiencies than observed for the system of monovalent sodium as shown in Fig. 4. This effect may be due to the higher mobility of the divalent specie, a greater selectivity of the resin toward the divalent specie, or a combination of both factors. Conversely for anions, the same study showed that the use of an SO_4^{2-} co-ion results in lower current efficiencies than when Cl is the co-ion, though mobilities (U) of the two anions are nearly identical [$U_{Cl} = 7.9 \times 10^{-4}$ cm^2·s^{-1}·V^{-1}, $U_{SO_4} = 8.3 \times 10^{-4}$ cm^2·s^{-1}·V^{-1} (33)]. This result is curious and deserves further consideration. It is likely that the substantial difference in the cathode electrode potentials of the two systems is responsible for this observation.

The system used to generate the results of Fig. 4 was initially a mixture of roughly 50/50 of the metal and salt in both the diluate and the concentrate streams. If linear mixing rules apply, it would be expected that the instantaneous current efficiency of this mixed system would lie approximately midway between the pure component current efficiencies. This is the result observed for this system, as the experimental data points are

seen to lie midway between the pure component curves. The linear mixing rule curve described by Eq. (11) (evaluated for diluate conditions) is seen to be in agreement with the experimental data.

Figures 5 and 6 also present results obtained for salt/metal systems. The system studied in Fig. 5 represents initial conditions in which the diluate is predominately salt, while the concentrate is roughly a 50/50 blend of salt and metal. Figure 6 represents a system in which the diluate is predominately metal, and the concentrate predominately salt. As seen in Figs. 5 and 6, there is agreement between the diluate-based linear mixing rule (11) and experimental data when high current efficiencies prevail (conditions of Eq. 8). In Fig. 5 the diluate is initially predominately salt and the mixed system current efficiency was observed to behave similar to the pure salt system where high current efficiency prevailed. In Fig. 6 the diluate is initially greater than 90% divalent metal. At high current efficiency the mixed system behavior is very close to that of a pure metal

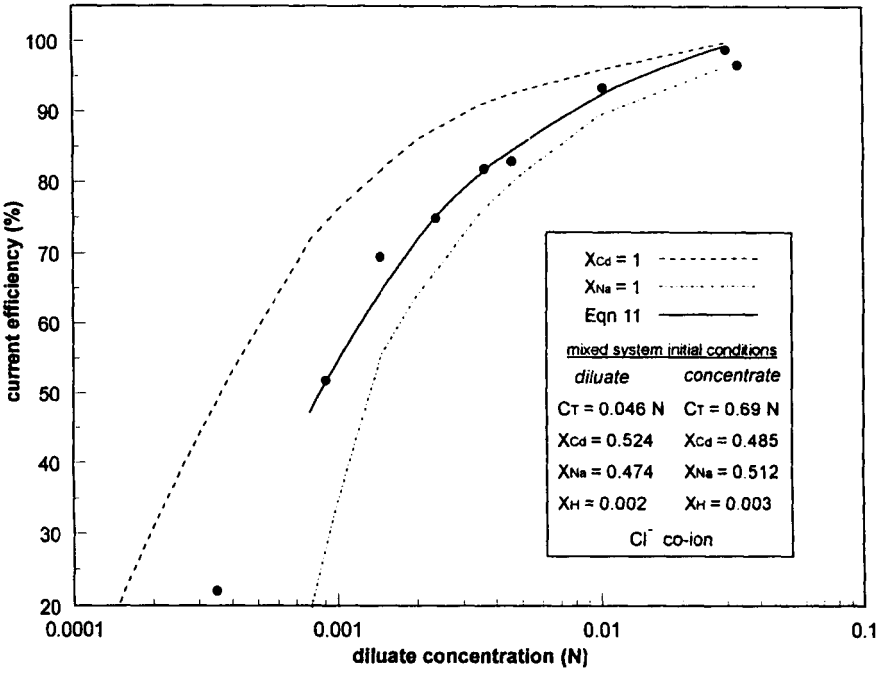

FIG. 4 Effect of diluate concentration on instantaneous current efficiency for a system initially with equal equivalents of salt and metal in the diluate and in the concentrate.

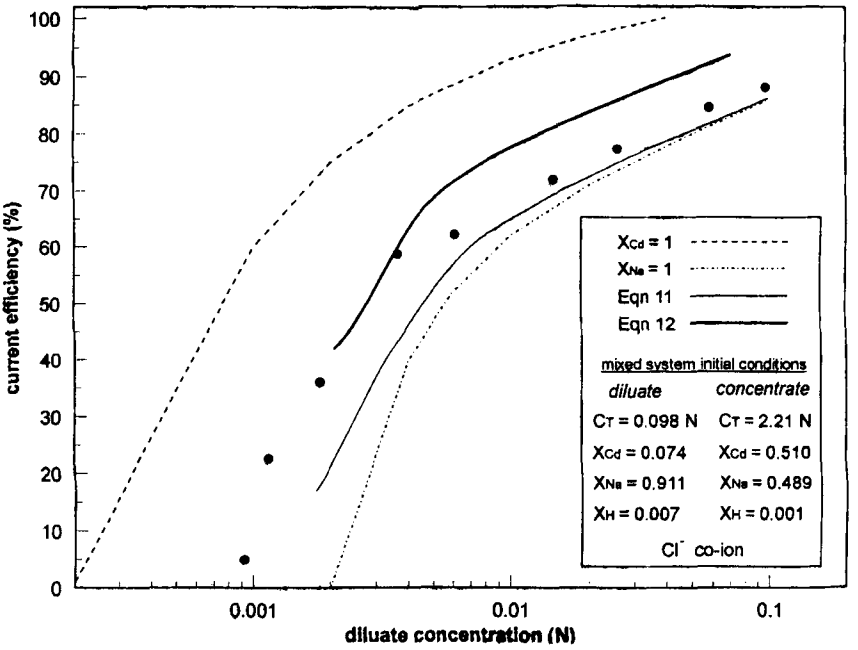

FIG. 5 Effect of diluate concentration on instantaneous current efficiency for a salt/metal system initially with a pure salt diluate and a concentrate of equal equivalents of salt and metal.

system. This behavior is predicted in both cases by the linear mixing rule based on the diluate conditions (Eq. 11) as was seen in Fig. 4.

At lower current efficiencies, neither diluate-based nor concentrate-based mixing rules provide an accurate fit for most of the previous results. Though the concentrate-based expressions approach the system behavior, it is obvious that neglecting the contribution of the diluate composition to η_t is an unacceptable oversimplification. The exact form of the fundamental equation should include the effect of water transport and water dissociation (as in the Nernst–Planck–Poisson equation). The Nernst–Planck–Poisson equation has been solved numerically for the electrodialysis separation of single species systems for various sets of limited operating conditions (29–32). These effects have been neglected and would be expected to have significant effects in this region for the binary systems.

In addition, the algebraic nature of the correlation results in the expres-

sion losing its intended meaning once the current efficiency of one of the pure components becomes zero. Thus, using Fig. 5 as an example, the correlations can only be applied above $C_D > 0.002$ N, the point at which η_i° for the pure salt system becomes zero. Below this concentration, salt in the mixed system does not make a contribution to the calculated current efficiency for the mixed system despite its presence in the experimental system.

In Fig. 6 the diluate is transported into a concentrate stream of practically pure salt. As the limiting separation is neared (at low current efficiency), the binary system begins to take on the characteristic current efficiency of the pure salt system. In this region the concentrate-based mixing rule is able to describe this behavior because the mixed system current efficiency approaches zero near the same diluate concentration as the pure salt system. The same is not true for the behavior of the system in Fig. 5 due to the algebraic limitations described above.

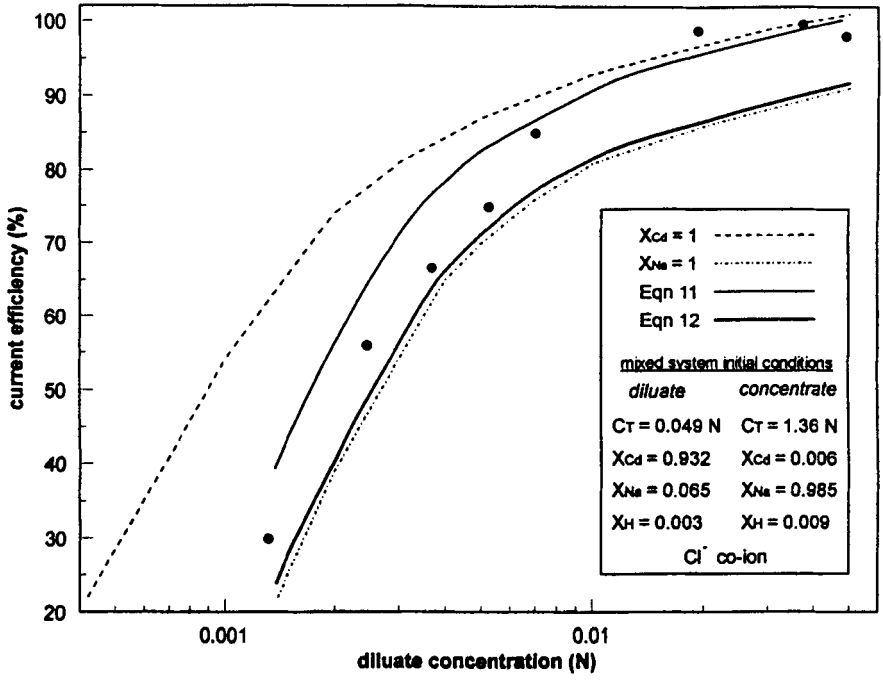

FIG. 6 Effect of diluate concentration on instantaneous current efficiency for a salt/metal system initially with a pure metal diluate and a pure salt concentrate.

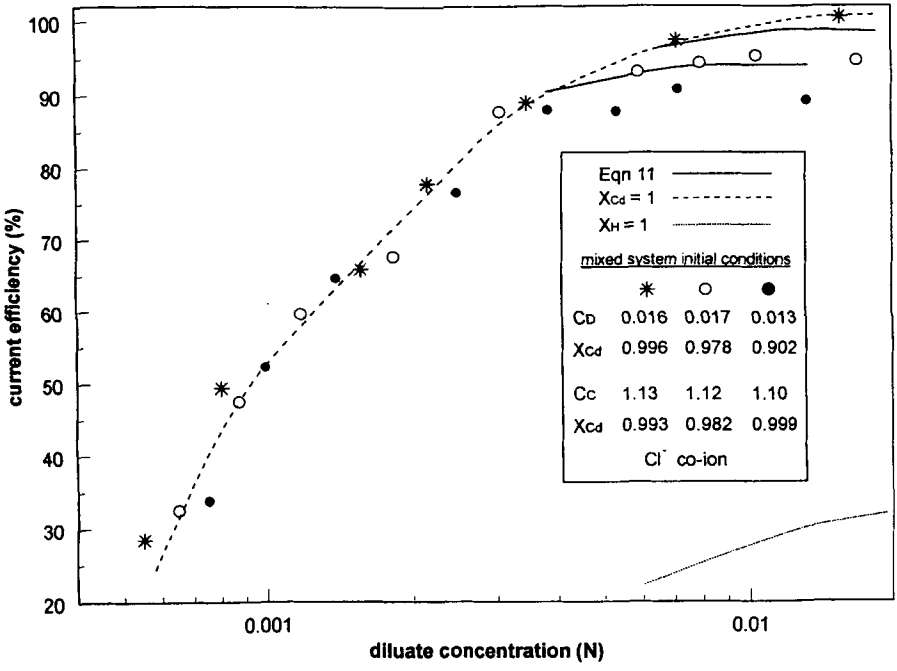

FIG. 7 Effect of diluate concentration on instantaneous current efficiency for acid/metal systems at variable concentrations of diluate acid.

Figures 7 and 8 illustrate the effect that acid has upon the overall current efficiencies for systems containing metal and salt, respectively. As indicated by the relative position of the pure acid ($X_H = 1$) curve with respect to the pure component monovalent salt ($X_{Na} = 1$) and divalent metal ($X_{Cd} = 1$) curves, overall current efficiencies for acid removal are extremely low compared to salt and metal current efficiencies. This is due to both the small size of the hydrogen ion and its high mobility [$u_H^+ = 3.625 \times 10^{-3}$ cm^2·s^{-1}·V^{-1}, $u_{Na}^+ = 5.193 \times 10^{-4}$ cm^2·s^{-1}·V^{-1} (33)]. The size of the hydrogen ion allows it to "leak" through anion-exchange membranes (co-ion intrusion) from the concentrate to the diluate, a transfer that is undesired and therefore results in a reduction in current efficiency. This dramatic effect on current efficiency caused by the addition of acid has also been observed by others (34). The linear mixing rule overestimates the current efficiency when substantial acid is present in the diluate in Figs. 7 and 8 but still provides reasonable approximations of the overall current efficiency when considering electrodialysis separations in regions

of commercial interest. Due to the algebraic limitations of the linear correlations discussed previously, Eq. (12) was not considered for the hydrogen ion, as these limitations are more pronounced with acid.

In Fig. 9, current efficiency results are presented for two mixed systems composed of acid, salt, and metal. The linear mixing rule based on diluate conditions overestimates the observed overall current efficiency when acid equivalent fractions in the diluate are significant (as was observed in Figs. 7 and 8), and underestimates current efficiencies at lower diluate concentrations. The reasons for the discrepancies follow the same reasoning as has already been presented.

In Figs. 4–9 the models described by Eqs. (11) and (12) failed when high concentration gradients were observed across the membrane (low current efficiencies). More sophisticated mixing rules can and need to be developed. However, there is currently insufficient data to test models which account for the nonlinearities observed here. The linear mixing rule is a predictive model and, therefore, defining the systems and regions for

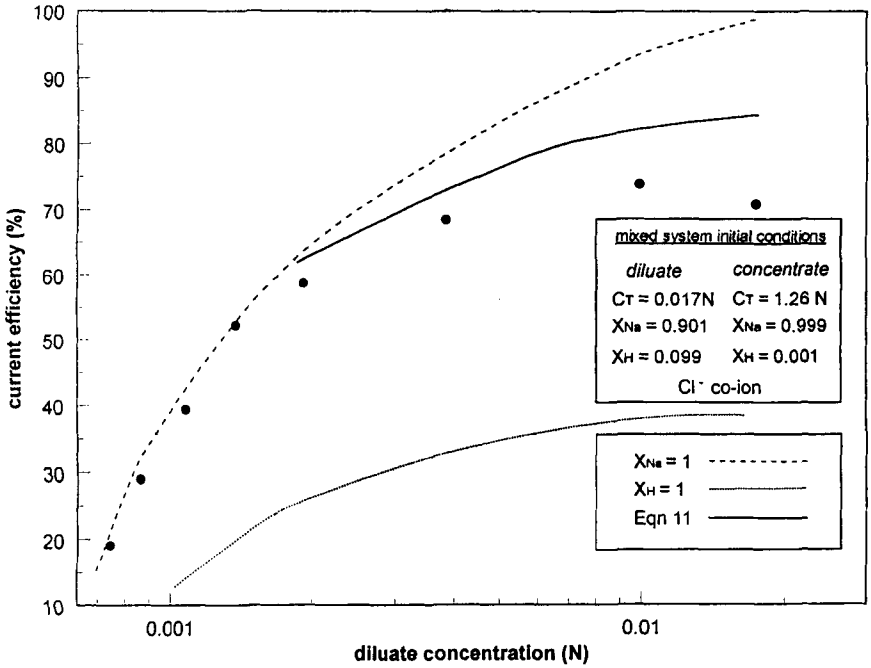

FIG. 8 Effect of diluate concentration on instantaneous current efficiency for an acid/salt system.

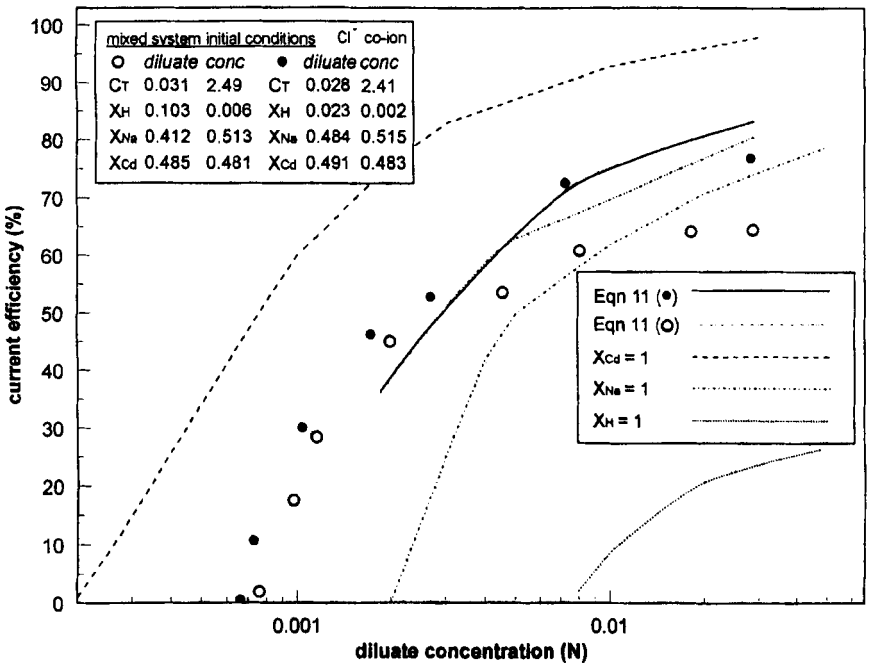

FIG. 9 Effect of diluate concentration on instantaneous current efficiency for acid/salt/metal systems at variable concentrations of diluate acid.

which it is valid seems valuable since it is so easy to use when it applies. The operating regions identified as applicable have the further advantage of being regions of commercial interest. Collection of additional mixed system data and development of improved models that combine both the diluate and concentrate concentrations into a single expression, as well as consider water transport, are future works in this area that will be performed. In addition, the algebraic complications associated with the mixing rules in which a specie pure component current efficiency goes to zero must be addressed to allow prediction in the low current efficiency region.

Figure 10 shows the apparent stack resistance versus diluate concentration for a number of the experimental runs that vary in solute nature and concentrate concentration. All nonsolution contributions to the apparent stack were kept consistent between experimental runs (including the contributions due to the electrode stream concentration), allowing changes in the apparent stack resistances for each run to be directly attributed to changes in the diluate and concentrate concentrations or the solute nature.

Figure 10 suggests apparent stack resistance is virtually unaffected by species compositions of the diluate and concentrate (both counterions and co-ions), but follows a strong correlation with the total Normal diluate concentration. All runs in Fig. 10 were at low acid concentration. Thus, prediction of the stack resistance for mixtures of monovalent salts and divalent metals can be based on measured resistance for a single monovalent salt or divalent metal compound.

The effect of acid concentration on the apparent stack resistance is seen in Fig. 11. This greater mobility of the hydrogen ion results in much lower electrical resistances. The resistances for these runs converge into a single line at low diluate concentrations. This is a consequence of the batch process. The point at which these lines converge represents the point at which the acid has been purged from the diluate and the system behaves like the system initially containing no additional acid.

Kitamoto and Takashima (35, 36) showed that membrane type has a significant effect upon design parameters in multicomponent systems. Thus trends observed here are expected to hold qualitatively for other

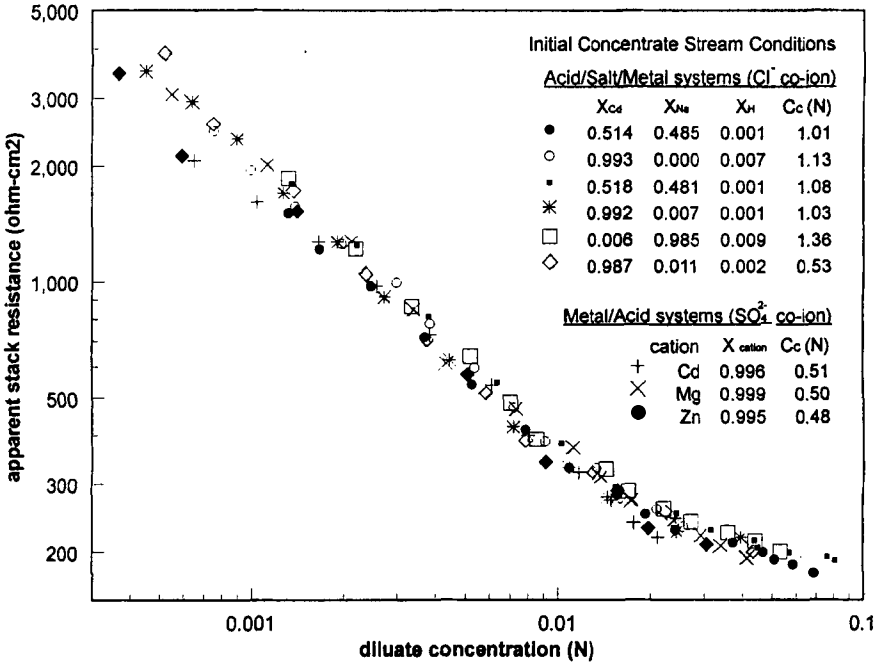

FIG. 10 Effect of diluate concentration on apparent stack resistance for salt/metal combinations at low diluate acid concentration.

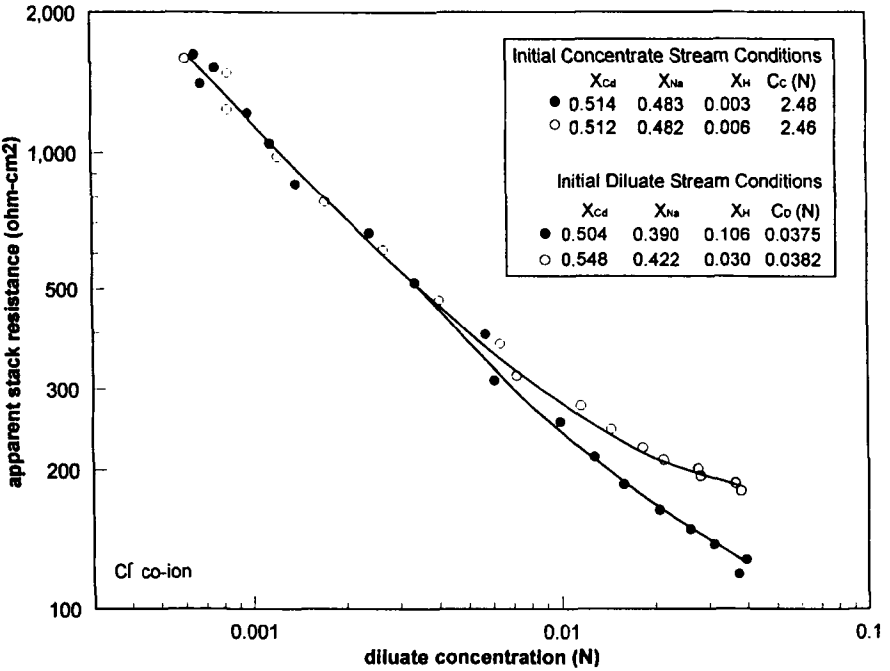

FIG. 11 Effect of diluate concentration on apparent stack resistance for salt/metal systems for low and for high diluate acid concentration.

ion-exchange membrane types. In addition, the hydrodynamics of the system have been maintained constant, and small changes in the flow characteristics can have considerable effects on the results (37).

SUMMARY OF CONCLUSIONS

- Metals, salts, and mixtures of these components can be efficiently removed from aqueous solutions of moderate pH by electrodialysis. As the pH of the solution is decreased, removal of the metal and salt cations becomes less efficient.
- Divalent cations have similar current efficiency and resistance under similar operating conditions, provided other effects (i.e., precipitation on or in a membrane) do not occur.
- Current efficiencies for binary salt/metal systems can be described in terms of linear combinations of the current efficiencies of the associated pure component systems when diffusive gradients across the membranes are small. Current efficiency for the mixed system can be

described from the pure component current efficiencies under these conditions based on the equivalent fractions of species present in the *diluate*.

- For monovalent salts, divalent metals, and salt/metal mixtures, apparent stack resistance is essentially independent of the solute nature and is a function of the total electrolyte concentration in the diluate (by Ohm's law).

ACKNOWLEDGMENTS

Financial support was provided by Bureau of Mines Grant G1125132-4001, the Oklahoma Mining & Minerals Resources Research Institute, and the Shell Development Co. The authors also thank Tam Van Tran, Phillip Wagner, and Robert Allison of Ionics, Inc. for technical data on the membranes used in this study.

NOMENCLATURE

A_π	effective cell pair area per cell pair (cm^2)
C_C	concentrate concentration (N)
$C_{i,C}$	concentrate concentration of cation i (N)
$C_{t,C}$	total concentrate concentration (N)
C_D	diluate concentration (N)
$C_{i,D}$	diluate concentration of cation i (N)
C_k	concentration of electrolyte specie k ($mol \cdot cm^{-3}$)
$C_{t,D}$	total diluate concentration (N)
ΔC_D	total change in diluate concentration during demineralization (N)
∇C_k	concentration gradient of species k ($mol \cdot cm^{-3} \cdot cm^{-1}$)
C	total electrolyte concentration (N)
D_k	diffusion coefficient of species k ($cm^2 \cdot s^{-1}$)
F	Faraday's constant (coulomb/equivalent)
i	current (amps)
I	equivalents of electric current (coulombs)
J_k	flux of species k ($mol \cdot s^{-1} \cdot cm^{-2}$)
n	number of cell pairs in membrane stack
R	universal gas constant ($J \cdot mol^{-1} \cdot K^{-1}$)
R_a	area specific apparent stack resistance (ohm-cm^2)
T	absolute solution temperature (K)
Δt	time between consecutive diluate samplings (s)
v	linear solution velocity ($cm \cdot s^{-1}$)

V_a	applied stack potential (V)
V_π	apparent stack potential per cell pair (V)
V_D	diluate volume contained in experimental unit (L)
$x_{i,C}$	equivalent fraction of cation i in the concentrate
$x_{i,D}$	equivalent fraction of cation i in the diluate
z_k	valence of specie k
α	effective cell pair area per unit flow rate of diluate ($cm^2 \cdot s/L$)
β	energy consumption per unit volume of diluate (J/L)
∇_ϕ	electrical potential gradient ($V \cdot cm^{-1}$)
η_I	overall instantaneous current efficiency
η_i°	overall instantaneous current efficiency for pure component i
η_I^{mix}	overall instantaneous current efficiency for electrolyte mixture

REFERENCES

1. L. H. Shaffer and M. S. Mintz, *Principles of Desalination*, 2nd ed. (K. S. Spiegler and A. D. K. Laird, Eds.), Academic Press, New York, NY, 1980, Chapter 6.
2. W. A. McRae,. *Desalination Technology, Developments and Practices* (Andrew Porteous, Ed.), Applied Science, 1983, Chapter 8.
3. P. M. Shah and J. F. Scamehorn, *Ind. Eng. Chem. Res.*, *26*, 269 (1987).
4. A. T. Cherif, C. Gavach, T. Cohen, P. Dagard, and L. Albert, *Hydrometallurgy*, *21*, 191–201 (1988).
5. J. B. Farrell and R. N. Smith, *Ind. Eng. Chem.*, *54*, 29 (1962).
6. M. J. Sweeny, *Summer Natl. AIChE Meeting, Seattle, WA, Paper No. 16b*, 1985.
7. T. Bhagat, *Water Pollut. Control*, *118*, 11 (1980).
8. S. M. Kulikov et al., *Desalination*, *104*, 107–111 (1996).
9. N. Boniardi, R. Rota, G. Nano, and B. Mazza, *Sep. Technol.*, *6*, 43–54 (1996).
10. O. L. Masanov, S. N. Dudnik, I. P. Turovskii, and A. A. Kulakov, *At. Energy*, *79*(1), 435–442 (1995).
11. G. Ramachandraiah et al., *Sep. Sci. Technol.*, *31*(4), 523–532 (1996).
12. D. H. Chen, S. S. Wang, and T. C. Huang, *Ibid.*, *31*(6), 839–856 (1996).
13. M. Pėrié and J. Pėrié, *Russ. J. Electrochem.*, *32*(2), 259–264 (1996).
14. H. Strathmann, H. J. Rapp, B. Bauer, and C. H. Bell, *Desalination*, *90*, 303 (1993).
15. K. N. Mani, *J. Membr. Sci.*, *58*, 117 (1991).
16. M. Paleologou et al., *Topical Conference Preprints, Vol. I: Recent Developments and Future Opportunities in Separations Technology*, AICHE Separations Division, November 12–17, 1995, Miami Beach, FL.
17. S. Novalic, J. Okwor, and K. D. Kulbe, *Desalination*, *105*, 277–282 (1996).
18. W. E. Katz, *Ibid.*, *23*, 31–40 (1979).
19. J. J. Schoeman, I. J. M. Buys, I. B. Schutte, and H. MacLeod, *Ibid.*, *70*, 407–429 (1988).
20. S. Sridhar, *J. Membr. Sci.*, *113*, 73–79 (1996).
21. D. G. Miller, *J. Phys. Chem.*, *70*(8), 2639–2658 (1966).
22. H. Miyoshi, *Sep. Sci. Technol.*, *31*(15), 2117–2129 (1996).
23. K. S. Spiegler, *Trans. Faraday Soc.*, *54*, 1408–1428 (1958).
24. H. Strathmann, *J. Sep. Process Technol.*, *5*(1), 1–13 (1984).

25. D. A. Rockstraw, J. F. Scamehorn, and E. A. O'Rear III, *J. Membr. Sci.*, *52*, 43 (1990).
26. J. A. Dean (Ed.), *Lange's Handbook of Chemistry*, 12th ed., McGraw-Hill, New York, NY, 1979.
27. K. L. Gering and J. F. Scamehorn, *Sep. Sci. Technol.*, *23*, 2231 (1988).
28. S. T. Hwang and K. Kammermeyer, *Techniques of Chemistry, Volume VII: Membranes in Separations*, Wiley, New York, NY, 1975.
29. M. Kh. Urtenov and V. V. Nikonenko, *Russ. J. Electrochem.*, *29*, 239 (1993).
30. I. Rubenstein and L. Shtilman, *J. Chem. Soc., Faraday Trans. II*, *75*, 231 (1979).
31. V. V. Nikonenko, V. I. Zabolotskii, and N. P. Gnusin, *Russ. J. Electrochem.*, *25*, 301 (1989).
32. A. V. Listovnichii, *Ibid.*, *25*, 1682 (1989).
33. A. J. Baird and L. R. Faulkner, *Electrochemical Methods: Fundamentals and Applications*, Wiley, New York, NY, 1980.
34. N. D. Pis'menskaya, *Russ. J. Electrochem.*, *32*(2), 277–283 (1996).
35. A. Kitamoto and Y. Takashima, *J. Chem. Eng. Jpn.*, *3*, 54 (1970).
36. A. Kitamoto and Y. Takashima, *Ibid.*, *3*, 285 (1971).
37. V. I. Zabolotskii and V. V. Nikonenko, *Russ. J. Electrochem.*, *32*(2), 223–230 (1996).

Received by editor August 29, 1996
Revision received November 1996